# Construction of $CoP_2$-$Mo_4P_3$/NF Heterogeneous Interfacial Electrocatalyst for Boosting Water Splitting

**Yafeng Chen [1,2], Ge Meng [1], Ziwei Chang [1], Ningning Dai [3], Chang Chen [1], Xinmei Hou [2,*] and Xiangzhi Cui [1,4,*]**

[1] The State Key Laboratory of High Performance Ceramics and Superfine Microstructures, Shanghai Institute of Ceramics, Chinese Academy of Sciences, Shanghai 200050, China
[2] Beijing Advanced Innovation Center for Materials Genome Engineering, Collaborative Innovation Center of Steel Technology, University of Science and Technology Beijing, Beijing 100083, China
[3] Shanghai Motor Vehicle Inspection Certification & Tech Innovation Center Co., Ltd., Shanghai 201805, China
[4] School of Chemistry and Materials Science, Hangzhou Institute for Advanced Study, University of Chinese Academy of Sciences, Hangzhou 310021, China
* Correspondence: houxinmeiustb@ustb.edu.cn (X.H.); cuixz@mail.sic.ac.cn (X.C.)

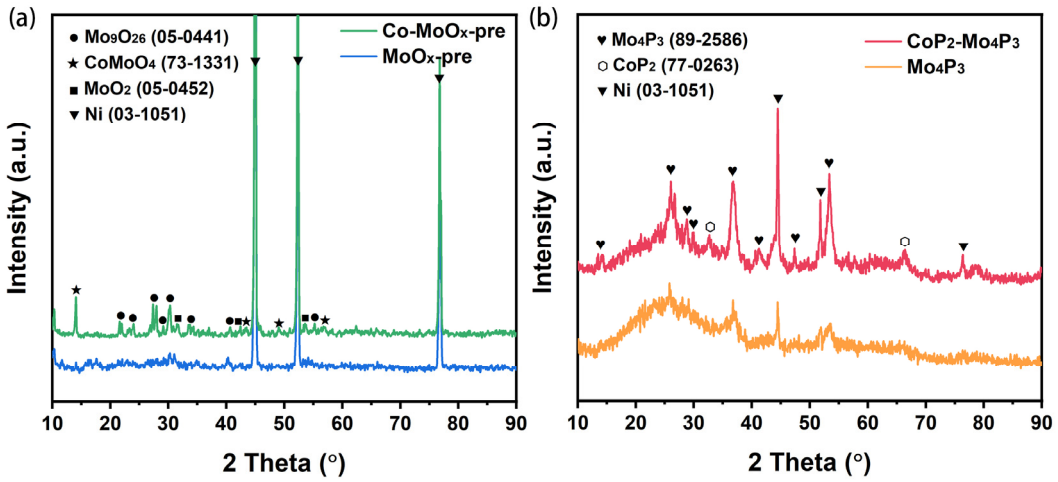


**Figure S1.** The XRD patterns of (a) Co-$MoO_x$/NF and $MoO_x$/NF precursors, and (b) $CoP_2$-$Mo_4P_3$/NF and $Mo_4P_3$/NF.

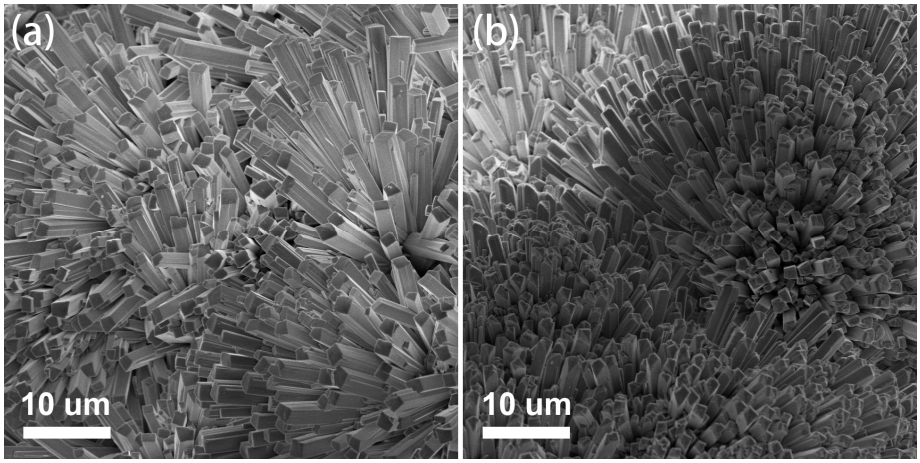


**Figure S2**. SEM images of (a) $MoO_x$/NF and (b) Co-$MoO_x$/NF precursors.

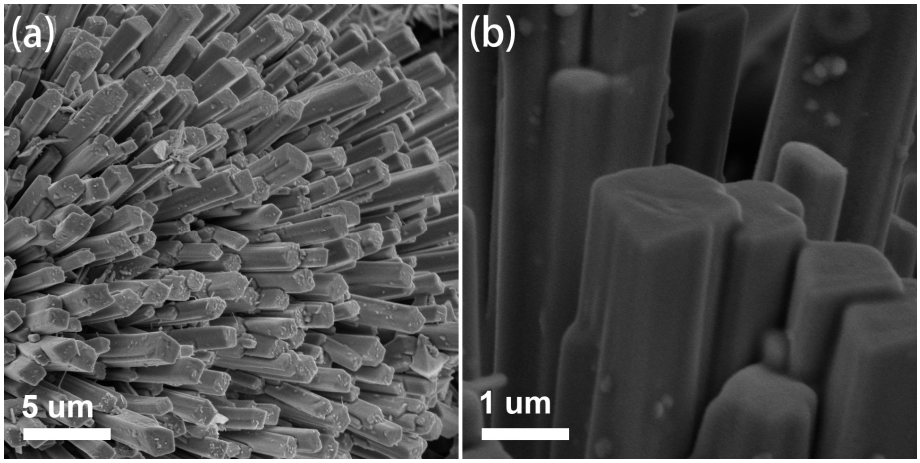


**Figure S3**. SEM images of $Mo_4P_3$/NF catalyst at different magnifications.

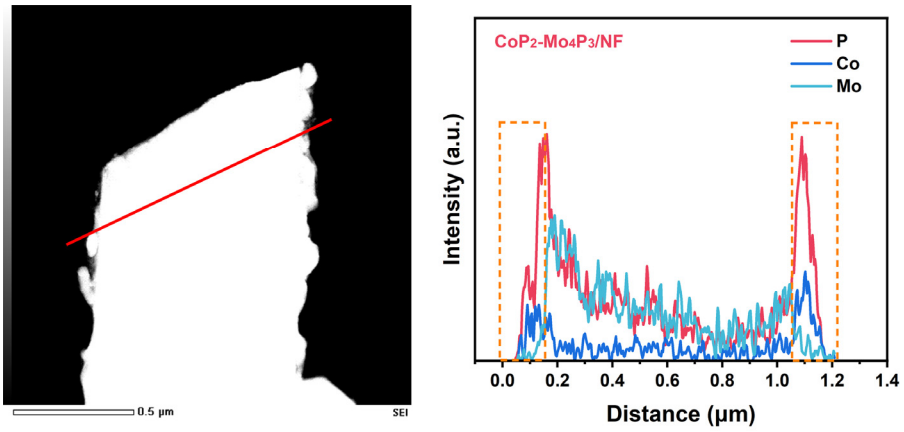


**Figure S4**. TEM-EDS line scanning image of $CoP_2$-$Mo_4P_3$/NF (left) and the corresponding elemental spectra (right).

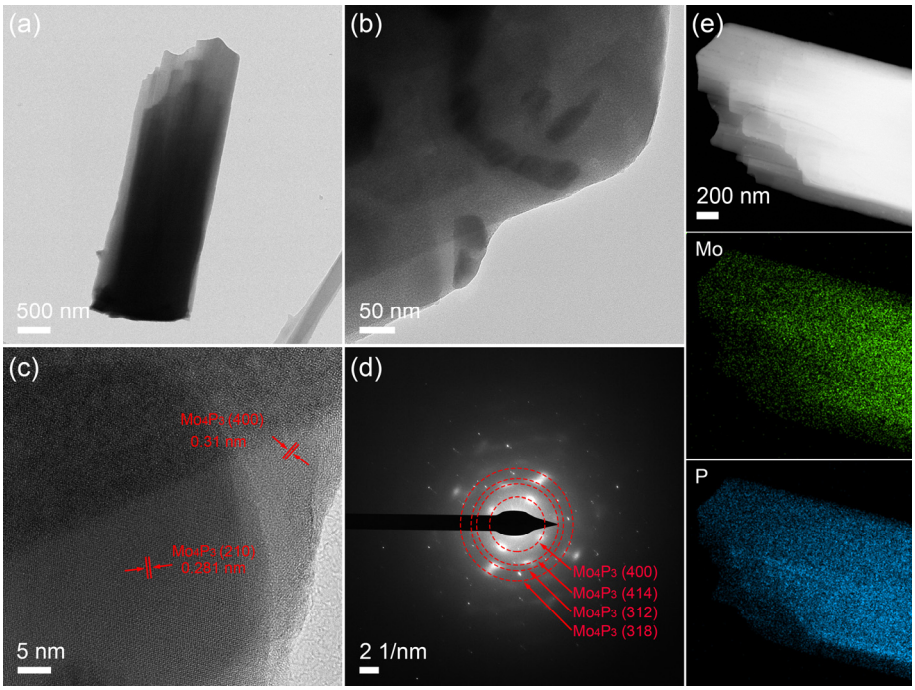


**Figure S5**. (a, b) TEM, (c) HRTEM, (d) SAED and (e) the corresponding elemental mapping images of $Mo_4P_3$/NF catalyst.

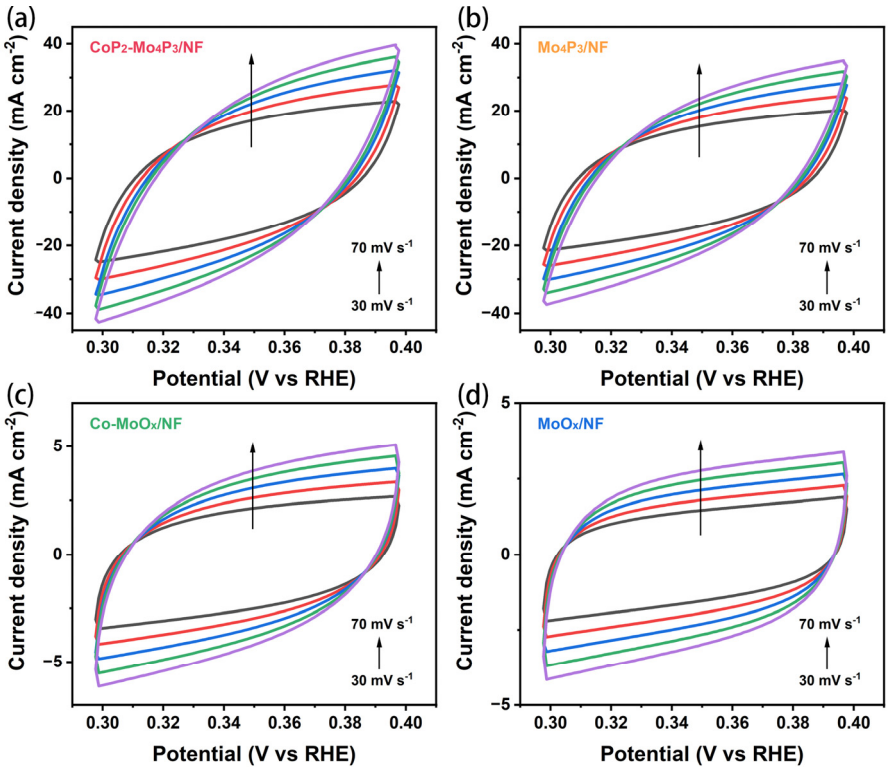


**Figure S6**. CV curves of (a) $CoP_2$-$Mo_4P_3$/NF, (b) $Mo_4P_3$/NF, (c) Co-$MoO_x$/NF and (d) $MoO_x$/NF at potential regions of 0.29-0.39 V (vs. RHE) with varied scan rates of 30-70 mV $s^{-1}$ in 1.0 M KOH.

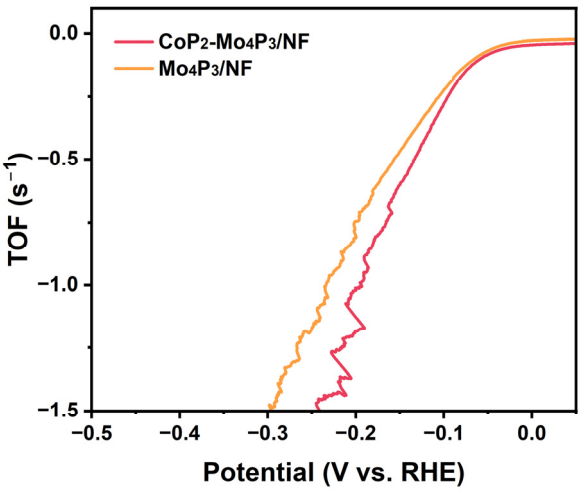


**Figure S7**. TOF curves of $CoP_2$-$Mo_4P_3$/NF and $Mo_4P_3$/NF catalysts.

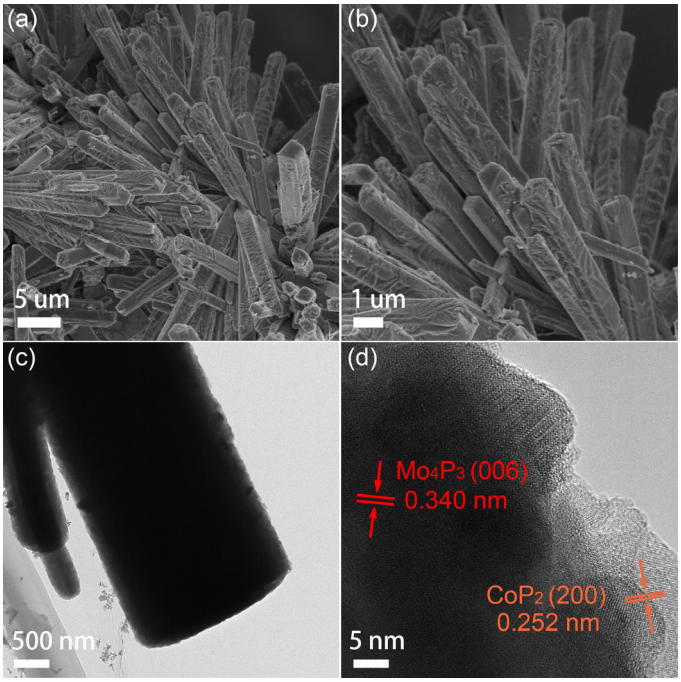


**Figure S8**. (a, b) SEM and (c, d) TEM images of $CoP_2$-$Mo_4P_3$/NF catalyst after HER stability experiment.

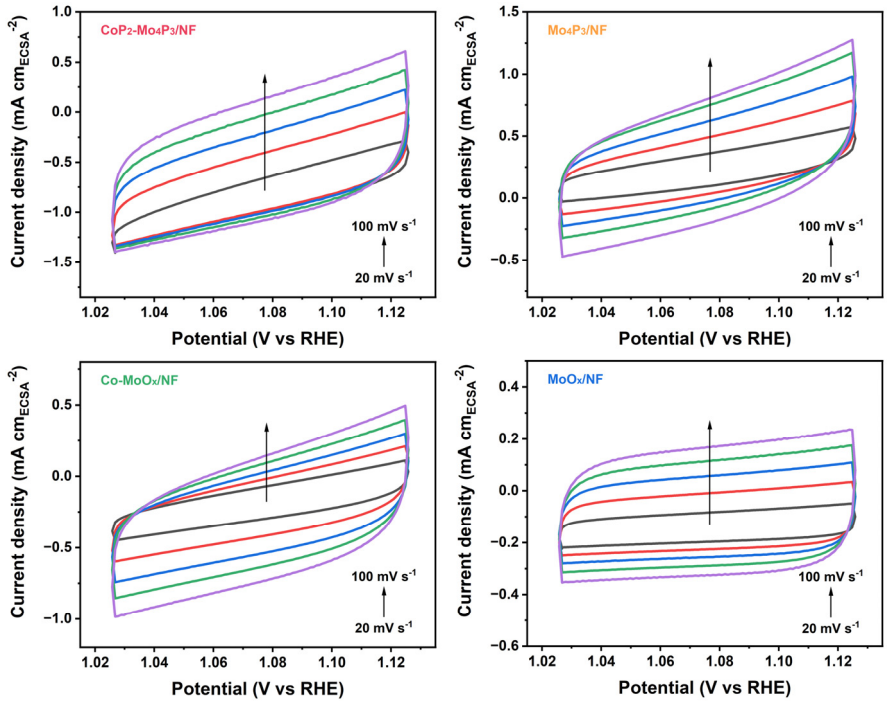


**Figure S9**. CV curves of (a) $CoP_2$-$Mo_4P_3$/NF, (b) $Mo_4P_3$/NF, (c) Co-$MoO_x$/NF and (d) $MoO_x$/NF at potential regions of 1.028-1.128 V (vs. RHE) with varied scan rates of 20-100 mV $s^{-1}$ in 1.0 M KOH.

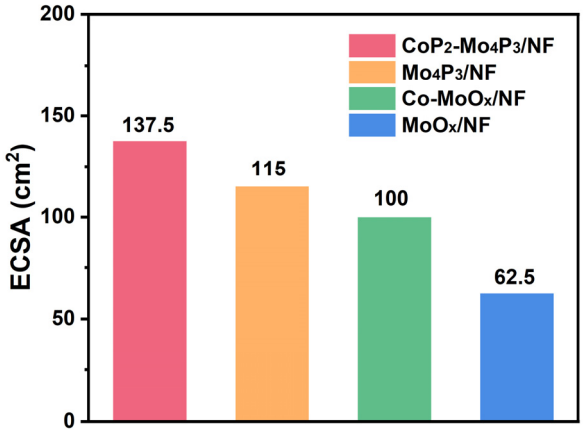


**Figure S10**. The calculated ECSA values of synthesized catalysts.

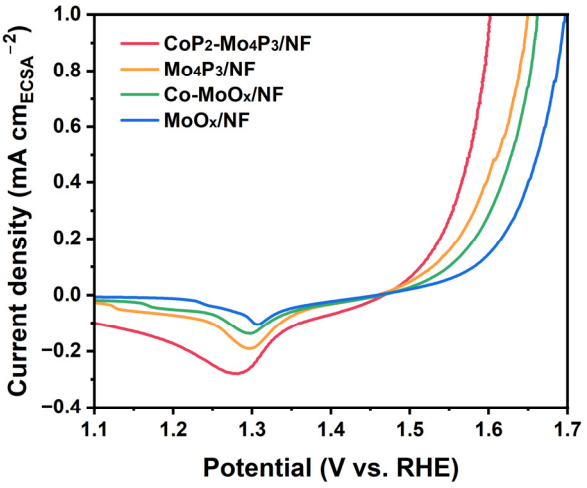


**Figure S11**. LSV curves normalized against ECSA.

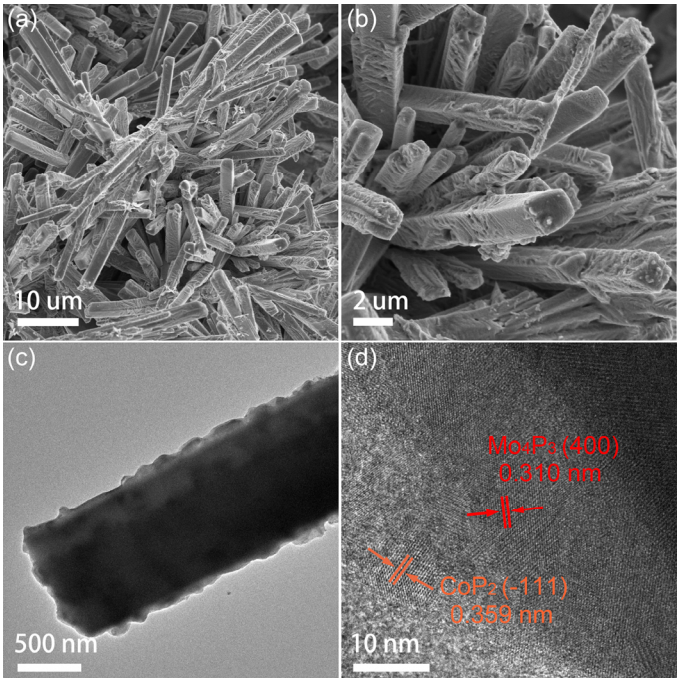


**Figure S12**. (a, b) SEM and (c, d) TEM images of $CoP_2$-$Mo_4P_3$/NF catalyst after OER stability experiment.

**Table S1**. EIS parameters of synthesized catalysts in 1.0 M KOH for HER.

| Materials | $R_s(\Omega)$ | $Q_1(S\cdot s^n)$ | $n_1$ | $R_{ct1}(\Omega)$ | $Q_2(S\cdot s^n)$ | $n_2$ | $R_{ct2}(\Omega)$ |
|---|---|---|---|---|---|---|---|
| **$CoP_2$-$Mo_4P_3$/NF** | 1.664 | 0.004 | 0.8 | 4.15 | 0.002 | 0.8 | 11.3 |
| **$Mo_4P_3$/NF** | 1.631 | 0.002 | 0.8 | 0.54 | 0.004 | 0.8 | 32.2 |
| **Co-$MoO_x$/NF** | 1.674 | 0.001 | 0.9 | 5.19 | 0.001 | 0.8 | 81.6 |
| **$MoO_x$/NF** | 1.584 | 0.005 | 0.8 | 2.69 | 0.001 | 0.8 | 96.1 |

**Table S2**. EIS parameters of synthesized catalysts in 1.0 M KOH for OER.

| Materials | Rs(Ω) | $Q_1(S \cdot s^n)$ | $n_1$ | $R_{ct1}(\Omega)$ | $Q_2(S \cdot s^n)$ | $n_2$ | $R_{ct2}(\Omega)$ |
|---|---|---|---|---|---|---|---|
| **$CoP_2$-$Mo_4P_3$/NF** | 1.514 | 0.096 | 0.9 | 0.49 | 0.295 | 0.67 | 7.57 |
| **$Mo_4P_3$/NF** | 1.492 | 0.197 | 0.7 | 0.42 | 0.839 | 0.89 | 9.59 |
| **Co-$MoO_x$/NF** | 1.674 | 0.200 | 0.8 | 0.12 | 0.260 | 0.80 | 21.2 |
| **$MoO_x$/NF** | 1.741 | 0.128 | 0.8 | 0.44 | 0.161 | 0.74 | 44.2 |

**Table S3**. Comparison of $CoP_2$-$Mo_4P_3$/NF||$CoP_2$-$Mo_4P_3$/NF with recently reported state-of-the-art OWS catalysts.

| Catalysts | Electrolyte | Cell voltage (V@j(mA $cm^{-2}$)) | Ref |
|---|---|---|---|
| **$CoP_2$-$Mo_4P_3$/NF** | 1.0 M KOH | 1.46@10<br>1.59@100 | This work |
| **Mo-NiS/$Ni(OH)_2$** | 1.0 M KOH | 1.50@10 | [1] |
| **P-NiMoP/NF** | 1.0 M KOH | 1.52@10 | [2] |
| **PRN-550** | 1.0 M KOH | 1.53@10 | [3] |
| **P-MoP/$Mo_2N$/NF** | 1.0 M KOH | 1.54@10 | [4] |
| **MoP/$Ni_2P$/NF** | 1.0 M KOH | 1.55@10 | [5] |
| **Co,Nb-$MoS_2$/$TiO_2$ HSs** | 1.0 M KOH | 1.59@10 | [6] |
| **MoP/NF** | 1.0 M KOH | 1.62@10 | [7] |
| **MoP@$Ni_3P$/NF** | 1.0 M KOH | 1.67@10 | [8] |
| **$Ru_1$/D-NiFe LDH** | 1.0 M KOH | 1.54@100 | [9] |
| **NiMoOx/NiMoS** | 1.0 M KOH | 1.62@100 | [10] |
| **P-NiMoP/NF** | 1.0 M KOH | 1.63@100 | [2] |
| **Ni/$Mo_2C$-NCS** | 1.0 M KOH | 1.66@100 | [11] |
| **MoP@NiCo-LDH/NF** | 1.0 M KOH | 1.7@100 | [12] |
| **Cr-CoP/CP** | 1.0 M KOH | 1.73@100 | [13] |
| **MoP-$Mo_2C$/NPC** | 1.0 M KOH | 1.77@100 | [14] |
| **FeNi LDH/$V_2CTx$/NF** | 1.0 M KOH | 1.78@100 | [15] |

## References


1. Zhang, H.; Xi, B.; Gu, Y.; Chen, W.; Xiong, S. Interface engineering and heterometal doping Mo-NiS/Ni(OH)$_2$ for overall water splitting. *Nano Res.* **2021**, *14*, 3466-3473.
2. Zhang, B.; Jiang, Z.; Shang, X.; Li, S.; Jiang, Z.-J. Accelerated hydrogen evolution reaction in $Ni_3P/MoP_2/MoO_2$ tri-phase composites with rich crystalline interfaces and oxygen vacancies achieved by plasma assisted phosphorization. *J. Mater. Chem. A* **2021**, *9*, 25934-25943.
3. Kim, M.; Park, J.; Ju, H.; Kim, J. Y.; Cho, H.-S.; Kim, C.-H.; Kim, B.-H.; Lee, S. W. Understanding synergistic metal–oxide interactions of in situ exsolved metal nanoparticles on a pyrochlore oxide support for enhanced water splitting. *Energy Environ. Sci.* **2021**, *14*, 3053-3063.
4. Gu, Y.; Wu, A.; Jiao, Y.; Zheng, H.; Wang, X.; Xie, Y.; Wang, L.; Tian, C.; Fu, H. Two-Dimensional Porous Molybdenum Phosphide/Nitride Heterojunction Nanosheets for pH-Universal Hydrogen Evolution Reaction. *Angew Chem Int Ed Engl* **2021**, *60*, 6673-6681.
5. Du, C.; Shang, M.; Mao, J.; Song, W. Hierarchical MoP/$Ni_2P$ heterostructures on nickel foam for efficient water splitting. *J. Mater. Chem. A* **2017**, *5*, 15940-15949.
6. Nguyen, D. C.; Luyen Doan, T. L.; Prabhakaran, S.; Tran, D. T.; Kim, D. H.; Lee, J. H.; Kim, N. H. Hierarchical Co and Nb dual-doped $MoS_2$ nanosheets shelled micro-$TiO_2$ hollow spheres as effective multifunctional electrocatalysts for HER, OER, and ORR. *Nano Energy* **2021**, *82*, 105750.
7. Jiang, Y.; Lu, Y.; Lin, J.; Wang, X.; Shen, Z. A Hierarchical MoP Nanoflake Array Supported on Ni Foam: A Bifunctional Electrocatalyst for Overall Water Splitting. *Small Methods* **2018**, *2*, 1700369.
8. Wang, F.; Chen, J.; Qi, X.; Yang, H.; Jiang, H.; Deng, Y.; Liang, T. Increased nucleation sites in nickel foam for the synthesis of MoP@$Ni_3P$/NF nanosheets for bifunctional water splitting. *Appl. Surf. Sci.* **2019**, *481*, 1403-1411.
9. Zhai, P.; Xia, M.; Wu, Y.; Zhang, G.; Gao, J.; Zhang, B.; Cao, S.; Zhang, Y.; Li, Z.; Fan, Z.; Wang, C.; Zhang, X.; Miller, J. T.; Sun, L.; Hou, J. Engineering single-atomic ruthenium catalytic sites on defective nickel-iron layered double hydroxide for overall water splitting. *Nat. Commun.* **2021**, *12*, 4587.
10. Zhai, P.; Zhang, Y.; Wu, Y.; Gao, J.; Zhang, B.; Cao, S.; Zhang, Y.; Li, Z.; Sun, L.; Hou, J. Engineering active sites on hierarchical transition bimetal oxides/sulfides heterostructure array enabling robust overall water splitting. *Nat. Commun.* **2020**, *11*, 5462.
11. Xu, Y.; Yang, J.; Liao, T.; Ge, R.; Liu, Y.; Zhang, J.; Li, Y.; Zhu, M.; Li, S.; Li, W. Bifunctional water splitting enhancement by manipulating Mo-H bonding energy of transition Metal-$Mo_2C$ heterostructure catalysts. *Chem. Eng. J.* **2022**, *431*, 134126.

12. Wang, T.; Wu, H.; Feng, C.; Zhang, L.; Zhang, J. MoP@NiCo-LDH on nickel foam as bifunctional electrocatalyst for high efficiency water and urea–water electrolysis. *J. Mater. Chem. A* **2020**, *8*, 18106-18116.
13. Li, W.; Jiang, Y.; Li, Y.; Gao, Q.; Shen, W.; Jiang, Y.; He, R.; Li, M. Electronic modulation of CoP nanoarrays by Cr-doping for efficient overall water splitting. *Chem. Eng. J.* **2021**, *425*, 130651.
14. Jiang, E.; Li, J.; Li, X.; Ali, A.; Wang, G.; Ma, S.; Kang Shen, P.; Zhu, J. MoP-$Mo_2C$ quantum dot heterostructures uniformly hosted on a heteroatom-doped 3D porous carbon sheet network as an efficient bifunctional electrocatalyst for overall water splitting. *Chem. Eng. J.* **2022**, *431*, 133719.
15. Yang, L.; Yang, T.; Chen, Y.; Zheng, Y.; Wang, E.; Du, Z.; Chou, K. C.; Hou, X. FeNi LDH/$V_2CT_x$/NF as Self-Supported Bifunctional Electrocatalyst for Highly Effective Overall Water Splitting. *Nanomaterials (Basel)* **2022**, *12*. 2640.